Optics Letters

Splitting spoof surface plasmon polaritons to different directions with high efficiency in ultra-wideband frequencies

Jun Wang,[1,3] Lei Zhao,[2,3,6] Zhang-Cheng Hao,[1,5,7] Xiaopeng Shen,[4] and Tie Jun Cui[1]

[1]State Key Lab of Millimeter-Waves, School of Information Science and Engineering, Southeast University, Nanjing, Jiangsu 211189, China
[2]School of Information and Control Engineering, China University of Mining and Technology, Xuzhou 221116, China
[3]Center for Computational Science and Engineering, School of Mathematics and Statistics, Jiangsu Normal University, Xuzhou, Jiangsu 221116, China
[4]Department of Physics, China University of Mining and Technology, Xuzhou 221116, China
[5]Purple Mountain Laboratories, Nanjing 211111, China
[6]e-mail: leizhao@cumt.edu.cn
[7]e-mail: zchao@seu.edu.cn

Received 24 April 2019; revised 30 May 2019; accepted 3 June 2019; posted 10 June 2019 (Doc. ID 365878); published 28 June 2019

An efficient method to split spoof surface plasmon polaritons (SSPPs) to different directions is proposed by designing a low-loss SSPP waveguide in an ultrawide frequency band. For this purpose, a coplanar-waveguide-based SSPP structure with double-row hole arrays etched on its middle line is first studied, which can be easily used to split the SSPP waves. Based on this method, a Y-shaped −3 dB SSPP power divider and its application on a Mach–Zehnder interferometer are presented. The experiment demonstrates that the proposed method splits the SSPP waves to different directions effectively in ultrawide frequencies (2.5–39.7 GHz) with good isolations, indicating that the proposed SSPP power divider can have good application on a Mach–Zehnder interferometer and plasmonic integrated circuits.

https://doi.org/10.1364/OL.44.003374

Spoof surface plasmon polaritons (SSPPs) are considered as a promising alternative wave mode for microwave applications, such as various antennas [1–3], surface plasmonic filters [4–13], and power dividers [14–23], due to their excellent performance of confining fields, wide bandwidth, and so on. In addition, they can be used to design miniaturized devices based on their characteristic of breaking through the diffraction limit. Thus, various SSPP devices are proposed based on slits, lumped elements, hole arrays, coplanar waveguide (CPW) designs, and some other structures [24–36].

As one of the key components in microwave circuits and communication systems, a power divider separates the power of the input signal into two output channels with equal or unequal power levels. The traditional method to split SSPP waves was to use gradient corrugation slit structures and specific flaring grounds [14–16]. However, the designs with flaring grounds are not beneficial to improve the transmission efficiency. Additionally, several SSPP metal grating splitters with finite thickness have also been studied numerically and experimentally [17–21], which achieve the division of two or more different frequencies. However, the isolation between the outputs of the above proposed SSPP splitters need to be further improved, and the fabrication cost is high. Furthermore, a SSPP-based lumped element Y-splitter and metal strip with hole array structures were proposed in Ref. [22] and Ref. [23], respectively. Unfortunately, the lumped element design is not a planar structure, and the performance of the hole array metal strip design needs to be perfected. Therefore, designing a high-efficiency, good-isolation, planar, low-cost SSPP-based power divider is technically very challenging. Nevertheless, a CPW-based SSPP waveguide filter was proposed in Ref. [29] recently, which uses periodic holes etched on the CPW stripline to realize low-pass transmission. Accordingly, the CPW-based SSPP waveguide filter is a good candidate method for future high performance SSPP-based power divider design and application on a Mach–Zehnder (MZ) interferometer.

In this Letter, an effective way to split the SSPP wave is proposed based on the design presented in Ref. [29]. Our purpose is to split the waves of the CPW-based SSPP waveguide filter. Hence, we first investigate a novel SSPP waveguide filter with double-row hole arrays etched on the CPW stripline, which realizes high transmission efficiency and similar performance with the single-row CPW-based SSPP waveguide filter. Based on these characteristics, a SSPP-based power divider is designed by employing the double-row hole arrays etched on the CPW stripline as input signal and splitting the input wave into output channels as Y-shaped by separating the double-row hole array in half along the center symmetrical axis. Additionally, a sharing ground for two output channels is added to improve the proposed Y-shaped power divider performance. The proposed splitting method is explained using dispersion relationships and electric field distributions with simulation software. Furthermore, the proposed splitting SSPP method can have

good application on a MZ interferometer. The proposed structure based on this method has the following features: 1) the efficiency of splitting SSPP wave transmission is high; 2) the isolation of the power divider is good; 3) the size of the design is compact; and 4) the design is very simple, flexible, and the fabrication cost is low.

The CPW-based SSPP waveguide filter proposed in Ref. [29] is a good plasmonic waveguide because of the tight field confinements and small propagation loss. However, etching single-row hole arrays is not beneficial to split the SSPP wave. Therefore, in order to split the SSPP wave conveniently, we first study a modified CPW-based SSPP design, which is designed by using the double-row hole arrays etched on the CPW, as shown in Fig. 1(a). The dashed box shows the unit cell of the proposed modified CPW-based design, and the length of the unit cell is marked as d. The performance of the proposed SSPP designs is simulated by commercial software CST. The dispersion curves of the modified CPW-based SSPP design are presented in Fig. 1(b), it is clear that the asymptotic frequency of the modified CPW-based SSPP design decreases with the increase in unit cell length. Moreover, Fig. 1(c) shows the simulated S-parameters of the proposed double-row hole arrays CPW-based SSPP waveguide filter, which illustrates the asymptotic frequency is about 42 GHz when $d = 2.5$ mm and agrees well with the corresponding dispersion curves presented in Fig. 1(b). The highest and lowest transmission coefficients of the CPW-based SSPP design are about −0.12 dB and −1 dB, respectively, which covers 1.6–41.7 GHz frequency band.

In order to further explain the operating principle of the modified CPW-based SSPP design, we present the simulated electric field distribution and magnitudes of energy at 20 GHz in Figs. 2(a) and 2(b), respectively. Moreover, Fig. 2(c) presents the power flow at y–z planes of the CPW-based SSPP design at 20 GHz, which shows that most of the EM fields are confined in 0.46λ (λ is the wavelength at 20 GHz). In Figs. 2(a)–2(c), we can see that the energy is limited on the slotted lines of CPW and periodic holes, which indicates that the modified CPW-based SSPP design can support SSPP waves propagating on its surface. Additionally, we can also find that the electric field distributions on the center of the middle of the CPW line are very sparse, which means that the SSPP waves may be able to propagate on semi-modified CPW-based SSPP

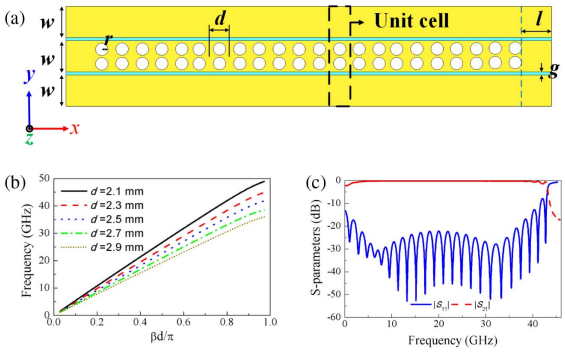

Fig. 1. (a) Structure of the proposed double-row hole arrays CPW-based SSPP design ($w = 3.6$ mm, $l = 4.71$ mm, $r = 0.71$ mm, $d = 2.5$ mm, and $g = 0.1$ mm). (b) Simulated dispersion curves of the CPW-based SSPP design with different d when r is fixed as 0.71 mm. (c) Simulated reflection and transmission coefficients of the proposed double-row hole arrays CPW-based SSPP design.

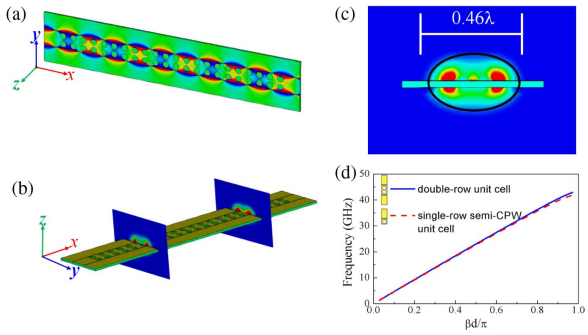

Fig. 2. (a) Electric field distribution on the x–y plane at 20 GHz when $d = 2.5$ mm. (b) Magnitudes of electric field on y–z plane at 20 GHz when $d = 2.5$ mm. (c) Power flow at y–z planes cutting the circular hole of the CPW-based SSPP design at 20 GHz. (d) Simulated dispersion curves of the double-row unit cell and single-row semi-CPW unit cell when $r = 0.71$ mm and $d = 2.5$ mm.

design. Therefore, the dispersion curves of the double-row unit cell and single-row semi-CPW unit cell when $r = 0.71$ mm and $d = 2.5$ mm are investigated and compared in Fig. 2(d), which shows that the two cases of unit cells have similar dispersion characteristics and asymptotic frequencies, making it possible to design a Y-shaped power divider by using the double-row hole arrays CPW-based SSPP waveguide filter and splitting the design in half along the center symmetrical axis.

Based on the dispersion relationships of the double-row and single-row semi-CPW unit cells, a Y-shaped SSPP power divider is proposed and researched, as shown in Fig. 3(a). The design consists of three parts: double-row CPW-based SSPP transmission part, single-row semi-CPW-based SSPP transmission part, and a sharing ground plane for two output channels. The width and gap of CPW striplines are marked as w and g, respectively. The radius of the hole slot is r, and the length of the unit cell is d. Moreover, the length and width of the sharing ground is marked as l_1 and w_1, respectively, and the distance with the semi-CPW-based SSPP part is g_1. The opening angle

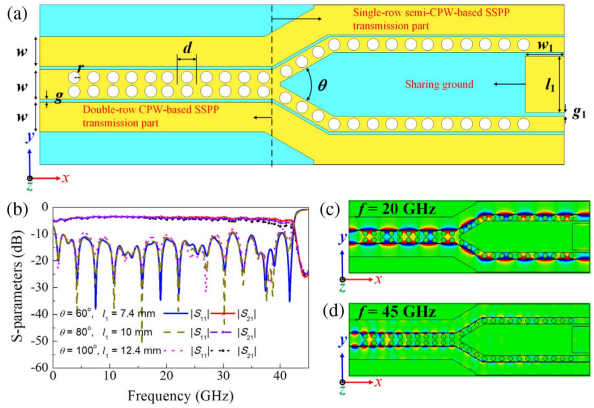

Fig. 3. (a) Structure of the proposed Y-shaped SSPP power divider ($w = 3.6$ mm, $w_1 = 5$ mm, $l_1 = 7.4$ mm, $r = 0.71$ mm, $d = 2.5$ mm, $g = 0.1$ mm, and $g_1 = 0.65$ mm). (b) Simulated S-parameters with different θ and l_1 values. (c) Simulated electric field distribution on the x–y plane at 20 GHz. (d) Simulated electric field distribution on the x–y plane at 45 GHz.

of the two single-row semi-CPW-based SSPP transmission parts is denoted as $\theta = 60°$. Figure 3(b) shows the performance of the proposed power divider for different θ with optimized l_1, which demonstrates that the proposed power divider can maintain a stable performance with changing θ. To verify the design concept and the proposed Y-shaped power divider performance, the simulated electric field distributions on the x–y plane are plotted in Figs. 3(c) and 3(d). Two frequencies (20 GHz and 45 GHz) are selected for comparison, which represent two typical frequencies below and above asymptotic frequency. It is clear that for 20 GHz, the electric fields are highly confined on the slot lines of the CPW, and the TM waves can propagate on branch metals of the proposed power divider. This feature makes sure that the waves can be divided equally into the output arms with almost no loss, which means that the SSPP wave can split as two equal channels effectively, whereas for 45 GHz, the SSPP field decays quickly along the propagation direction, which implies that the SSPP wave cannot be confined because its operation frequency is higher than the asymptotic frequency.

Additionally, a sharing ground plane is added into the Y-shaped power divider to improve its performance. The S-parameters with and without the sharing ground are presented in Fig. 4, which shows that the $|S_{11}|$ and $|S_{21}|$ with the sharing ground are better than ones without the sharing ground. The simulated bandwidth (for $|S_{11}| < -10$ dB and $|S_{21}| > -4.5$ dB) of the proposed Y-shaped SSPP power divider with the sharing ground is about 176.3% (2.5–39.7 GHz), and the highest $|S_{21}|$ is up to −3.35 dB. We observe that the asymptotic frequency is about 42 GHz, satisfying the dispersion result analyzed in Fig. 1(b). Moreover, the isolation of ports 2 and 3 is below −15 dB, from 4 GHz to 45 GHz. Based on these simulated results, we can conclude that the proposed method can divide the input SSPP waves into two equal output waves in an ultra-wideband with a low transmission loss and good isolation.

MZ interferometers control optical and electric signals in sub-millimeter scale integrated circuits [33]. The key component of the MZ interferometer is the −3 dB power divider, which is able to obtain different signal output responses by adding different dielectric constant materials on one of the power divider arms. Therefore, we can use the MZ interferometer to estimate the dielectric constant of the unknown material. The schematic diagram of the MZ interferometer is shown in Fig. 5(a); the design comprises two symmetrical power dividers and a reference substrate (assuming the dielectric constant is ε_r and the thickness is 1 mm). When we add the different reference substrates at the upper arm of the MZ interferometer,

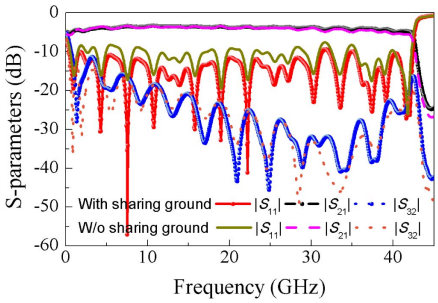

Fig. 4. Simulated S-parameters with and without sharing ground of the proposed Y-shaped SSPP power divider.

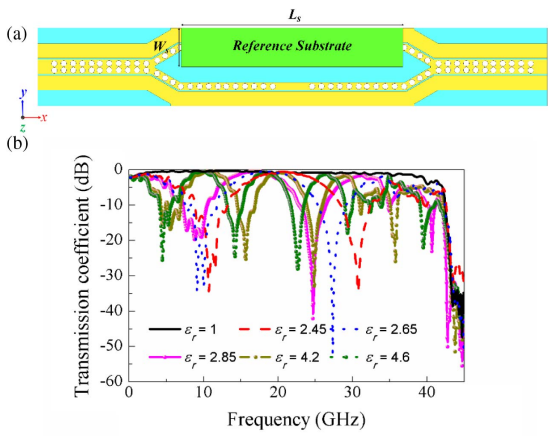

Fig. 5. (a) Configuration of the proposed MZ interferometer; the designed parameters of the reference substrate are $L_s = 60$ mm, $W_s = 10$ mm, and the thickness is 1 mm. (b) Simulated transmission coefficient ($|S_{21}|$) of the MZ interferometer with different dielectric constants of the reference substrate.

the phase of the upper arm will be changed, and the total output response can be obtained by the superposition of two arm signals. Therefore, we can obtain different output signals by changing the reference substrate. Figure 5(b) presents the simulated transmission coefficient ($|S_{21}|$) of the MZ interferometer with different dielectric constants of the reference substrate (ε_r is selected as 1, 2.45, 2.65, 2.85, 4.2, and 4.6, respectively). It is clear that the MZ interferometer has different signal output responses when the dielectric constant of the reference substrate changes, and the resonant frequencies shift to lower frequencies as the dielectric constant of the reference substrate increases.

In order to verify the proposed method to split SSPP waves, we fabricated and measured prototypes of a SSPP power divider and MZ interferometer, as shown in Figs. 6 and 7. The designs are printed on the 0.5 mm F4B substrate with $\varepsilon_r = 2.65$, loss tangent $\tan\delta = 0.0015$, and the thickness of the metallic strips is 0.035 mm. To demonstrate the high-efficiency transmissions quantitatively, Fig. 6(b) shows the simulated and

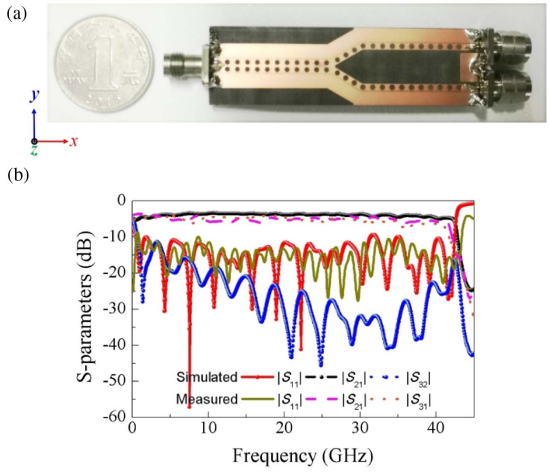

Fig. 6. (a) Photograph of the fabricated Y-shaped SSPP power divider. (b) Measured and simulated S-parameters of the proposed Y-shaped SSPP power divider.

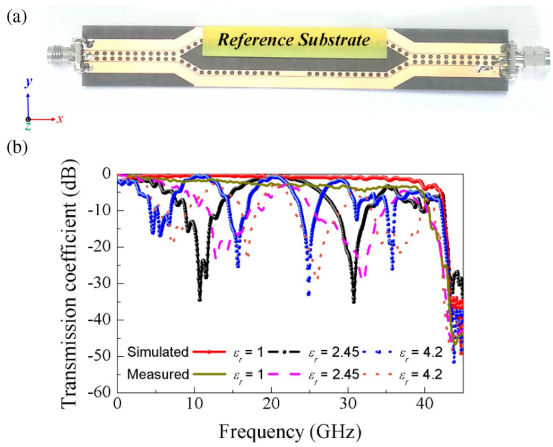

Fig. 7. (a) Photograph of the fabricated MZ interferometer. (b) Measured and simulated transmission coefficient ($|S_{21}|$) of the proposed MZ interferometer.

measured results of the proposed Y-shaped SSPP power divider. It is clear that the simulated bandwidth (for $|S_{11}| < -10$ dB and $|S_{21}| > -4.5$ dB) is 2.5–39.7 GHz, and the measured results agree well with the simulated ones. Meanwhile, Fig. 7(b) presents the measured results of the MZ interferometer (dielectric constant of the reference substrate ε_r is selected as 1, 2.45, and 4.2, respectively), which agree will with the simulated results shown in Fig. 5(b). Moreover, the difference between the measured and simulated results at some frequencies and the frequencies of the MZ interferometer have a slight shift to the higher frequencies, which are maybe caused by the subminiature A (SMA) soldering and measurement tolerances.

In conclusion, we present a feasible method to split SSPP waves at microwave frequencies. The method is first investigated from a special CPW-based SSPP waveguide and then verified by designing a Y-shaped SSPP power divider, which is designed by separating the double-row hole array CPW design in half along the center symmetrical axis. Finally, an application on the MZ interferometer based on the power divider is also presented. The proposed method of splitting SSPPs is explained using the dispersion curves and electric field distributions. Prototypes of the proposed power divider and MZ interferometer have been fabricated and measured to verify the physical concept. The measured results have good agreement with the simulated ones, which indicates that the proposed splitting method is helpful in designing future SSPP devices at microwave frequency band.

Funding. National Natural Science Foundation of China (NSFC) (61372057, 61571117, 61631007, 61771226); Natural Science Foundation of the Jiangsu Higher Education Institutions of China (18KJA110001); Natural Science Foundation of Xuzhou of China (KC18003).

REFERENCES

1. A. Kianinejad, Z. N. Chen, L. Zhang, W. Liu, and C. W. Qiu, IEEE Trans. Antennas Propag. **64**, 2094 (2016).
2. Y. J. Han, Y. F. Li, H. Ma, J. F. Wang, D. Y. Feng, S. B. Qu, and J. Q. Zhang, IEEE Antennas Wireless Propag. Lett. **65**, 1187 (2017).
3. Q. L. Zhang, Q. F. Zhang, and Y. F. Chen, IEEE Trans. Antennas Propag. **16**, 3014 (2017).
4. L. L. Liu, Z. Li, C. Q. Gu, P. P. Ning, B. Z. Xu, Z. Y. Niu, and Y. J. Zhao, J. Appl. Phys. **116**, 013501 (2014).
5. H. F. Ma, X. P. Shen, Q. Cheng, W. X. Jiang, and T. J. Cui, Laser Photon. Rev. **8**, 146 (2014).
6. B. C. Pan, Z. Liao, J. Zhao, and T. J. Cui, Opt. Express **22**, 13940 (2014).
7. L. Zhao, X. Zhang, J. Wang, W. H. Yu, J. D. Li, H. Su, and X. P. Shen, Sci. Rep. **6**, 36069 (2016).
8. Z. Liao, J. Zhao, B. C. Pan, X. P. Shen, and T. J. Cui, J. Phys. D **47**, 315103 (2014).
9. H. C. Zhang, S. Liu, X. P. Shen, L. H. Chen, L. M. Li, and T. J. Cui, Laser Photon. Rev. **9**, 83 (2015).
10. W. J. Zhang, G. Q. Zhu, L. G. Sun, and F. J. Lin, Appl. Phys. Lett. **106**, 021104 (2015).
11. D. W. Zhang, K. Zhang, Q. Wu, G. H. Yang, and X. J. Sha, Opt. Lett. **42**, 002766 (2017).
12. Q. X. Xiao, B. J. Yang, and Y. J. Zhou, J. Appl. Phys. **118**, 233112 (2015).
13. Y. J. Zhou and Q. X. Xiao, J. Appl. Phys. **121**, 123109 (2017).
14. X. Gao, L. Zhou, X. Y. Yu, W. P. Cao, H. O. Li, H. F. Ma, and T. J. Cui, Opt. Express **23**, 23270 (2015).
15. S. Y. Zhou, J. Y. Lin, S. W. Wong, F. Deng, L. Zhu, Y. Yang, Y. J. He, and Z. H. Tu, Sci. Rep. **8**, 5947 (2018).
16. Y. L. Wu, M. X. Li, G. Y. Yan, L. Deng, Y. A. Liu, and Z. Ghassemlooy, AIP Adv. **6**, 105110 (2016).
17. Y. J. Zhou, Q. Jiang, and T. J. Cui, Opt. Express **19**, 5260 (2011).
18. Y. J. Zhou, X. X. Yang, and T. J. Cui, J. Appl. Phys. **115**, 123105 (2014).
19. J. Shibayama, J. Yamauchi, and H. Nakano, Electron. Lett. **51**, 352 (2015).
20. Y. J. Zhou and T. J. Cui, Appl. Phys. Lett. **98**, 221901 (2011).
21. Y. L. Wu, Z. Zhuang, L. Deng, and Y. A. Liu, Sci. Rep. **6**, 24495 (2016).
22. S. Passinger, A. Seidel, C. Ohrt, C. Reinhardt, A. Stepanov, R. Kiyan, and B. N. Chichkov, Opt. Express **16**, 14369 (2008).
23. B. G. Xiao, S. Kong, J. Chen, and M. Y. Gu, Opt. Quantum Electron. **48**, 179 (2016).
24. S. A. Maier, S. R. Andrews, L. Martin-Moreno, and F. J. Garcia-Vidal, Phys. Rev. Lett. **97**, 176805 (2006).
25. Y. J. Zhou, Q. Jiang, and T. J. Cui, Appl. Phys. Lett. **99**, 111904 (2011).
26. B. Z. Xu, Z. Li, L. L. Liu, J. Xu, C. Chen, P. P. Ning, X. L. Chen, and C. Q. Gu, Opt. Lett. **40**, 004683 (2015).
27. Q. Gan, Z. Fu, Y. J. Ding, and F. J. Bartoli, Phys. Rev. Lett. **100**, 256803 (2008).
28. Y. J. Guo, K. D. Xu, and X. H. Tang, Opt. Express **26**, 10589 (2018).
29. J. Wang, L. Zhao, Z. C. Hao, and T. J. Cui, Appl. Phys. Lett. **113**, 071101 (2018).
30. Z. Li, L. L. Liu, H. Y. Sun, Y. H. Sun, C. Q. Gu, X. L. Chen, Y. Liu, and Y. Luo, Phys. Rev. Appl. **7**, 044028 (2017).
31. J. Yang, S. X. Zhou, C. Hu, W. W. Zhang, X. Xiao, and J. Zhang, Laser Photon. Rev. **8**, 590 (2014).
32. D. W. Zhang, K. Zhang, Q. Wu, R. W. Dai, and X. J. Sha, Opt. Lett. **43**, 003176 (2018).
33. L. L. Liu, Z. Li, C. Q. Gu, P. P. Ning, B. Z. Xu, Z. Y. Niu, and Y. J. Zhao, Opt. Express **22**, 10675 (2014).
34. R. A. S. Ferreira, C. D. S. Brites, C. M. S. Vicente, P. P. Lima, A. R. N. Bastos, P. G. Marques, M. Hiltunen, L. D. Carlos, and P. S. André, Laser Photon. Rev. **7**, 1027 (2013).
35. L. L. Liu, Z. Li, C. Q. Gu, B. Z. Xu, P. P. Ning, C. Chen, J. Yan, Z. Y. Niu, and Y. J. Zhao, Opt. Lett. **40**, 001810 (2015).
36. K. D. Xu, Y. J. Guo, and X. J. Deng, Opt. Express **27**, 4354 (2019).